ELSEVIER

Contents lists available at ScienceDirect

Virology

journal homepage: www.elsevier.com/locate/yviro



The structure of *Sinorhizobium meliloti* phage Φ M12, which has a novel T=19l triangulation number and is the founder of a new group of T4-superfamily phages $^{1/2}$



M. Elizabeth Stroupe a,b,*, Tess E. Brewer Duncan R. Sousa a,b, Kathryn M. Jones a

- ^a Department of Biological Science, Florida State University, Biology Unit I, 230A, 91 Chieftan Way, Tallahassee, FL, 32306-4370, United States
- b Institute of Molecular Biophysics, Florida State University, 91 Chieftan Way, Tallahassee, FL, 32306-4370, United States

ARTICLE INFO

Article history:
Received 12 July 2013
Returned to author for revisions
23 September 2013
Accepted 10 November 2013
Available online 6 January 2014

Keywords:
Bacteriophage
ΦM12
Myovirus
Sinorhizobium meliloti
T=19
Icosahedral

ABSTRACT

 Φ M12 is the first example of a T=19l geometry capsid, encapsulating the recently sequenced genome. Here, we present structures determined by cryo-EM of full and empty capsids. The structure reveals the pattern for assembly of 1140 HK97-like capsid proteins, pointing to interactions at the pseudo 3-fold symmetry axes that hold together the asymmetric unit. The particular smooth surface of the capsid, along with a lack of accessory coat proteins encoded by the genome, suggest that this interface is the primary mechanism for capsid assembly. Two-dimensional averages of the tail, including the neck and baseplate, reveal that Φ M12 has a relatively narrow neck that attaches the tail to the capsid, as well as a three-layer baseplate. When free from DNA, the icosahedral edges expand by about 5 nm, while the vertices stay at the same position, forming a similarly smooth, but bowed, T=19l icosahedral capsid.

© 2013 Elsevier Inc. All rights reserved.

Introduction

The collection of bacteriophages found across varying environmental niches is incredibly diverse, despite the apparent molecular simplicity of a minimal 'organism' composed of nucleic acid and protein. Indeed, each newly sequenced genome highlights the diversity, which manifests in differing genome organizations, variations of capsid and tail proteins, and the array of accompanying enzymes encoded by the phage genetic material (Holmes, 2011). Despite their diversity, tailed bacteriophages with icosahedrally symmetric capsids appear to have evolved from a common ancestor. The structurally conserved capsid protein serves as the single protein of which the highly symmetric shell is composed, regardless of the asymmetric unit used to form the icosahedron (Veesler and Cambillau, 2011).

To date, fewer than 50 unique 3D structures of tailed icosahedral bacteriophage capsids have been deposited in the 3DEM or PDB databases (www.ebi.ac.uk or www.pdb.org), and even fewer of these phages have an accompanying complete genomic sequence. This is a minuscule percentage of the uncharacterized

E-mail address: mestroupe@bio.fsu.edu (M.E. Stroupe).

phages that can be found infecting host bacteria that live in environments as different as the gut is from the soil. Despite their shared icosahedral geometry and common major capsid protein, no two capsid structures are identical.

One of the prototypical members of the *Myoviridae* family is the dsDNA, *Escherichia coli*-infecting phage T4, which has an elongated capsid and a contractile tail whose baseplate and tail fibers confer host specificity (Fokine et al., 2004; Leiman et al., 2004). Historically, T4 has served as a model system for understanding the molecular biology of phages and their host prokaryotes, as well as the structural basis for the phage lifecycle (Adriaenssens et al., 2012; Chen et al., 2007; Sullivan et al., 2010). T4-superfamily phages within this family include a broad range of contractile-tail, icosahedral-capsid phage whose host range spans from enterobacteria to cyanobacteria (Dreher et al., 2011; Mann et al., 2005; Sullivan et al., 2005, 2010; Weigele et al., 2007).

Phage Φ M12 belongs in this extended class of T4-superfamily phages and infects the soil bacterium *Sinorhizobium meliloti* 1021, an important environmental bacterium because of its ability to establish a nitrogen-fixing symbiosis within root nodules. Genomic analysis has revealed that Φ M12 represents a new lineage of dsDNA, T4-superfamily phages (Brewer et al., in press). We have determined the 3D structure of Φ M12 to 1.8 nm resolution with cryogenic single particle electron microscopy and tomography. Φ M12 has a T=19 laevo (T=191) architecture, with shallow turrets at its 5-fold vertices. A narrow neck connects the capsid to its long, helically symmetric contractile tail. The tail ends with a base plate

 $^{^{*}(}See$ also accompanying manuscript: The genome, proteome and phylogenetic analysis of Sinorhizobium meliloti phage $\Phi \text{M12},$ the founder of a new group of T4-superfamily phages).

^{*}Corresponding author at: Department of Biological Science, Florida State University, 91 Chieftan Way, Tallahassee, FL 32306-4370, USA.

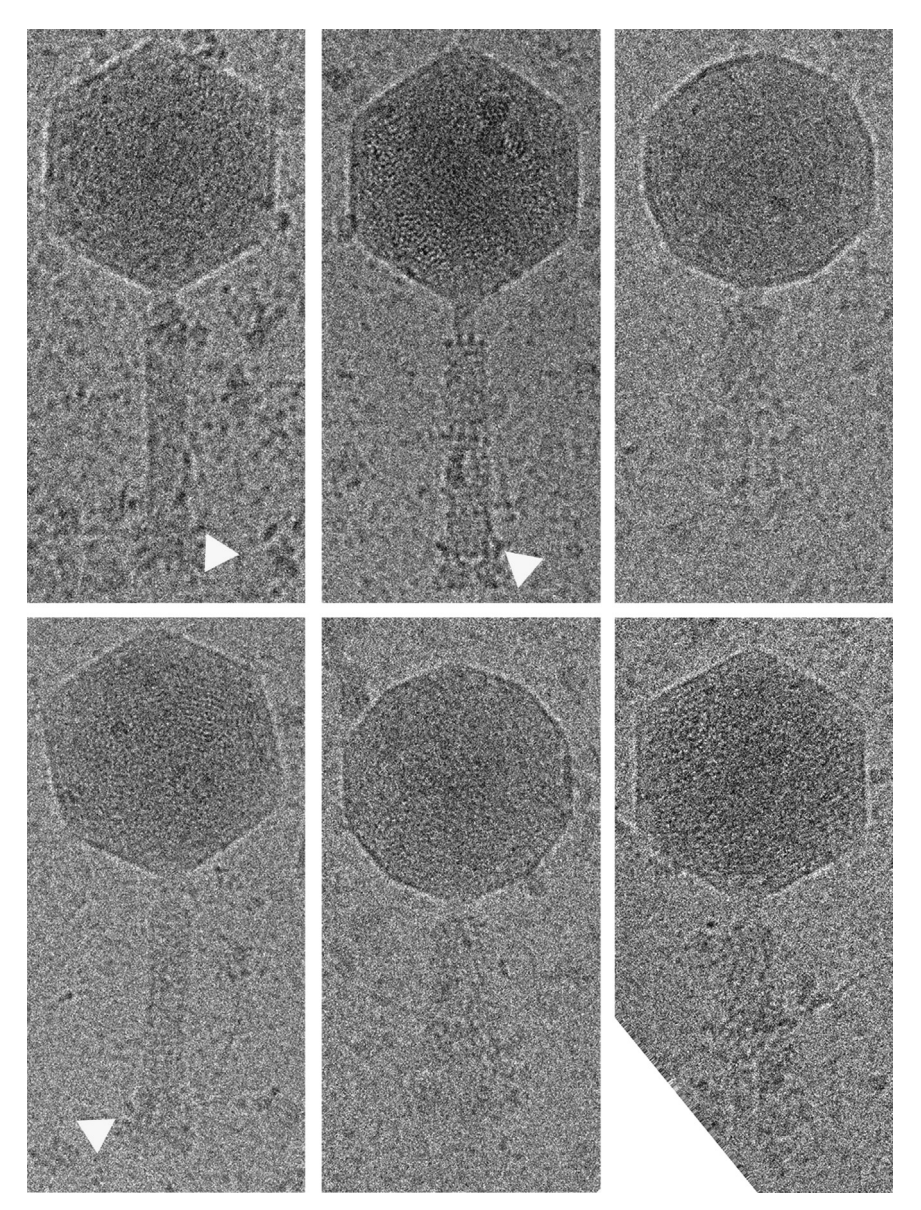


Fig. 1. Raw images of full icosahedral ΦM12 phage capsids with heterogeneous, contractile tails. The arrows point to the short, heterogeneous tail fibers.

that does not have as many tail fibers as some other phages, including the related cyanophage Syn9 (Weigele et al., 2007). DNA is tightly packed in the capsid, but small changes resulting in relaxation at the 3-fold symmetry axes occur when the capsid does not have packaged DNA. This expansion is similar to one empty state of the HK97 virus (Duda et al., 2009).

Results and discussion

New class of phage

The Φ M12 phage falls into a new class of T4-superfamily tailed bacteriophage whose genome contains elements of other well-characterized phages that infect either cyanobacteria or enterobacteria (Brewer et al., in press). Φ M12 is also unique in that it has the first reported T=191 capsid shell.

ΦM12 has an isometric, icosahedral capsid, a narrow neck, a long contractile tail, and a baseplate that has few obvious tail fibers (Fig. 1). The internally packed genomic dsDNA is apparent in the full capsids, both in the raw images and in slices through the tomographic reconstructions (Figs. 1 and S2). The

ΦM12 phage capsid is 100 nm in diameter and the fully extended tail is 90 nm from the neck to the top of the baseplate. The baseplate is about 30 nm in diameter and 17.5 nm thick, resulting in an overall height of 207.5 nm from the top of the capsid to the tip of the tail. Heterogeneity of the tail shows a continuum of contraction states, from the full extended to the fully contracted (Fig. 1). As the phage tail contracts, it becomes bushier than when fully extended.

Capsid structure

 Φ M12 is an isometric T=19l virion with short turrets sitting atop elevated pentamers that contribute an additional 2.5 nm each to its width, for a total diameter of 105 nm (Fig. 2). The surface of the capsid is smooth but continuous, with shallow dimples punctuating the surface that trace the hexamer of major coat protein (Fig. 3A). The pentamers protrude from the smooth surface underneath the turrets about 1.5 nm away from the flat hexamers. The empty capsid is also T=19l with a smooth, dimpled surface similar to that of the full capsid (Fig. 3B).

The turrets that sit at the top of each elevated pentamer are shaped like inverted pentagonal pyramids, where the top of the

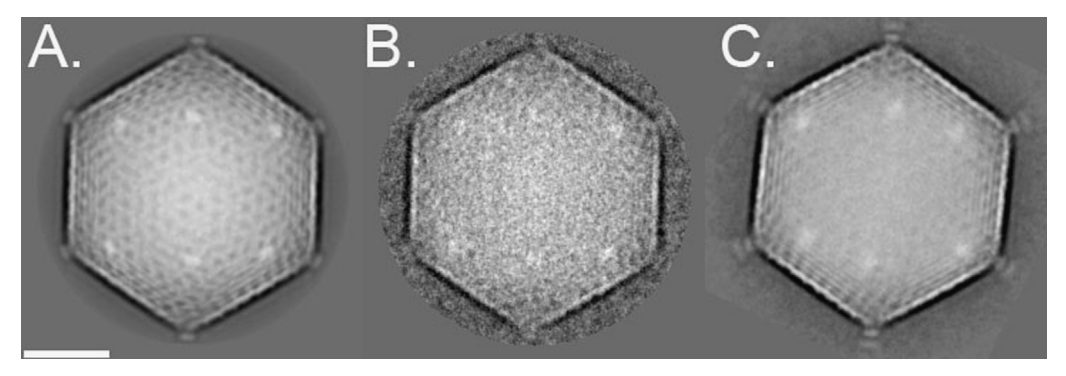


Fig. 2. (A) Projection, (B) Reference-based class average, and (C) Reference-free class average show the smooth, turreted capsid packed with DNA. The scale bar is 30 nm.

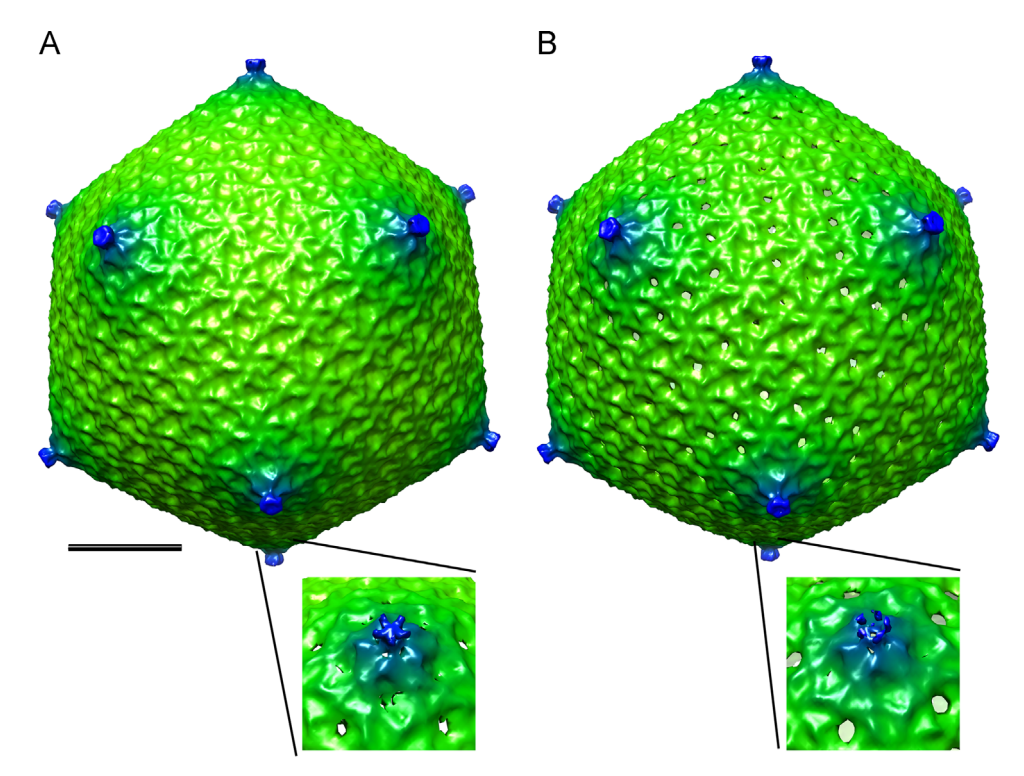


Fig. 3. (A) Reconstruction of full Φ M12 virions reveals a smooth surface punctuated by dimples that outline the hexameric subunit. Inset: lower contoured isosurface shows the 5-fold symmetry of the turrets atop a protruding pentamer. (B) Reconstruction of empty Φ M12 virions has holes at the pseudo and real 2-fold symmetry axes. Inset: lower contoured isosurface of the stretched turret. Both structures are colored according to the distance of the point from the center of the capsid, where the green is 50 nm radius from the center of the particle and blue is at 57 nm radius. The scale bar is 25 nm.

turret is the pentagonal base of the pyramid (Fig. 3). Each turret has a diameter of about 5 nm at the maximal width and is about 4 nm wide at the junction with the pentamer of the capsid. The turrets are linked to the capsid through five buttress-like projections and the broad top of the turret is composed of five fingers offset from the contours of the pentamer that curl away from the capsid (Fig. 3A, inset). The empty capsid has similar finger-like projections but somewhat less pronounced buttresses (Fig. 3B, inset). The identity of the turret protein is unknown.

T=19l creates an expansive viral capsid

One thousand hundred forty copies of Φ M12's major coat protein assemble to make 180 hexamers and 11 pentamers around the smooth surface of the icosahedron (Fig. 4A). Fifty-five of those 1140 major coat proteins compose the pentamer and could be a different polypeptide than that which makes up the hexamer, perhaps coming from a domain of the unidentified turret protein, but there is no gp24-like molecule in the genome analogous to the

gp24 of T4, which makes up its pentameric vertices (Brewer et al., in press; Fokine et al., 2005). The 12th pentamer would be replaced by the tail assembly, which is averaged out in this icosahedrally averaged structure.

The asymmetric unit contains one subunit of an A_5 pentamer and three unique hexamers (BCDEFG, HIJKLM, and NOPQRS), to achieve the T number of 19 and *laevo* hand (Fig. 4B and C). With this arrangement of subunits, there are seven different sets of trimer interactions that uniquely define the symmetry of the capsomere: ABG, cFm, DLN, EhS, ipR, jKO, and Qqq (lower case letters demark subunits provided by symmetry mates of the 19-mer asymmetric unit). Although the surface of the Φ M12 capsid is quite smooth (Figs. 3 and 4), at more stringent density contours the points of trimer interactions that hold together the asymmetric unit show stronger density than the comparable quasi 2-fold positions, which are marked by weaker density (Fig. 4A and D).

The capsid encloses a volume of 1.9×10^6 nm³ to encapsulate an approximately 200 kilobase pair genome. Syn9, which infects

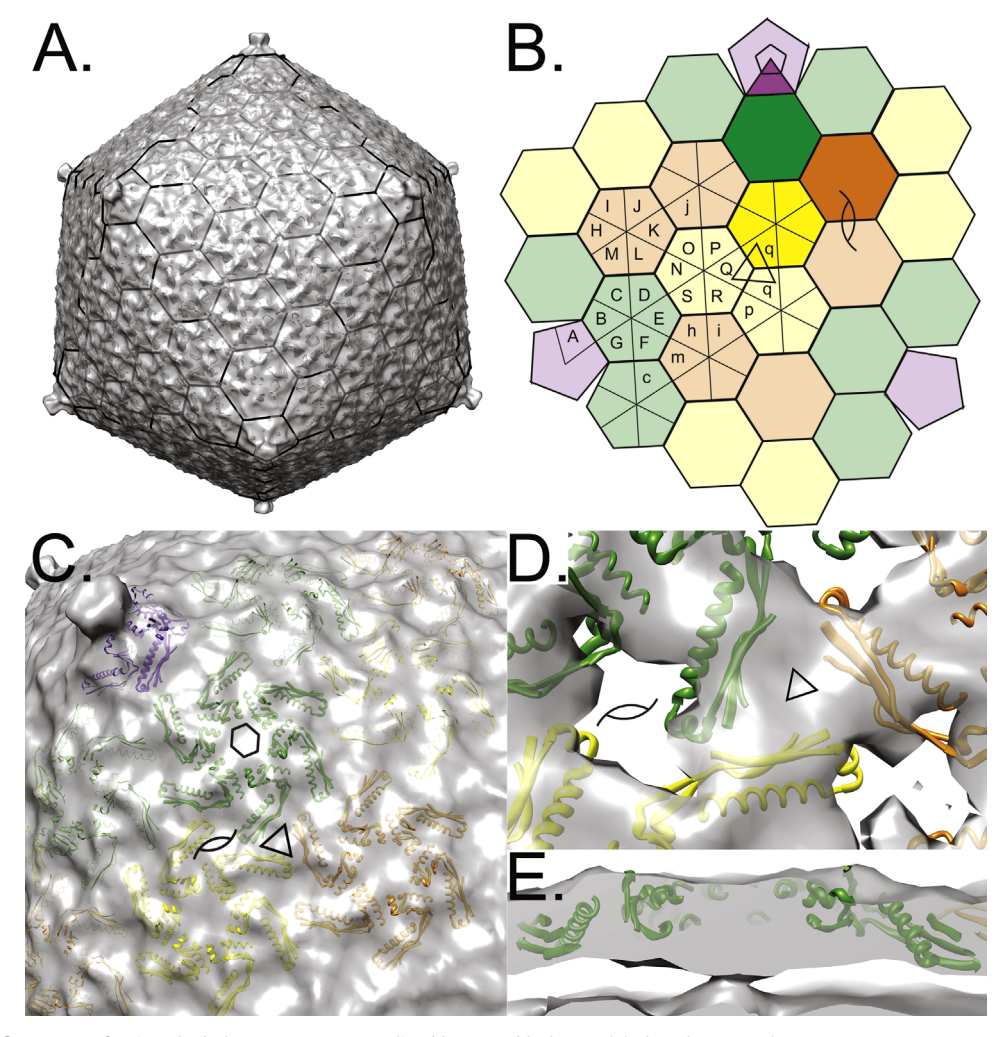


Fig. 4. (A) Φ M12 is the first report of an icosahedral T=19 geometry, outlined here as a black cage. (B) Three hexamers (green – BCDEFG, orange – HIJKLM yellow – NOPQRS) and one subunit from the adjacent pentamer (purple – A_5) make up the T=19 asymmetric unit. Seven different trimer interactions describe the packing of the gp23 monomer within this geometry. Capital letters denote the elements of the asymmetric unit, whereas lowercase denote elements from neighboring symmetry mates that complete the trimers. (C) A model of the core elements of the HK97 capsid protein (PDB code 3J1A (Shen et al., 2012)) fits into the smooth, narrow frame of the capsid to the resolution of the reconstruction with pseudo 6-fold (hexagon), pseudo 3-fold (triangle) and pseudo 2-fold (half moons). (D) The strong trimer interface and weaker dimer interface. The pseudo 3-fold symmetry axis relating the three hexamers of the asymmetric unit is demarked by a triangle and the pseudo 2-fold symmetry axis, which relates two of the hexamers, is demarked by half moons. The pseudo hexamer is demarked by a hexagon. (E) A thin slice through the center of a hexamer showing the central density that is not filled by the minimal model of the HK97 core elements, pointing to the variable I domain/E loop as important in its assembly.

Synechococcus, is the closest icosahedral cyanophage to Φ M12 whose genome and 3D structure have been determined (Weigele et al., 2007). Syn9 has a genome of 180 kilobase pairs enclosed in an isometric T= 16 capsid of diameter 88 nm (Weigele et al., 2007). Its internal volume, 1.4×10^6 nm³, is on the order of the volume of the T4 prolate head, whose genome is about 170 kilobase pairs (Miller et al., 2003; Weigele et al., 2007). The T= 191 asymmetric unit adds 180 subunits to the slightly smaller T=16 capsid, increasing the number of subunits by 19% to accommodate a genome that is 11% longer (for a single copy). The added subunits increase the internal volume by 36%, though, suggesting that packing coat protein monomers into a T= 191 arrangement is more efficient at creating internal space for storing a large genome than its T=16 relative.

HK97-like gp23 and the T=19l assembly

Capsid proteins protect the viral genome from the environment as the virus passes from one host to another. Icosahedral coats are capable of assembling according to the principles of quasi-equivalence, as described by Casper and Klug over a half century ago

(Caspar and Klug, 1962). Many capsid proteins from diverse bacteriophages and viruses share a small number of common folds that assemble into the characteristic hexamers and pentamers required for the icosahedral coats, suggesting that most virions have diverged from a small number of progenitors (Veesler and Cambillau, 2011). The HK97-like major coat protein is one such fold, found in a range of bacteriophages and viruses including its namesake HK97 (Wikoff et al., 2000), T4 (Fokine et al., 2005), Syn9 (Weigele et al., 2007), and ΦM12 (Fig. 5A).

ΦM12 ORF 65 was easily identified as ΦM12's major coat protein (Brewer et al., in press). The conserved gp23 fold can accommodate icosahedral capsids with different asymmetric units in diverse virions because it is structurally variable (Veesler and Cambillau, 2011). A structurally conserved core, composed of the common central elements has been identified (Shen et al., 2012) and its molecular model was docked into the ΦM12 envelope with the Chimera Fit in Map feature (Pettersen et al., 2004). The smooth density map fits the contours of the central fold with discrepancies at the quasi 3-fold and quasi 6-fold symmetry axes in the asymmetric unit, where the minimal model leaves unfilled additional density (Fig. 4C–E).

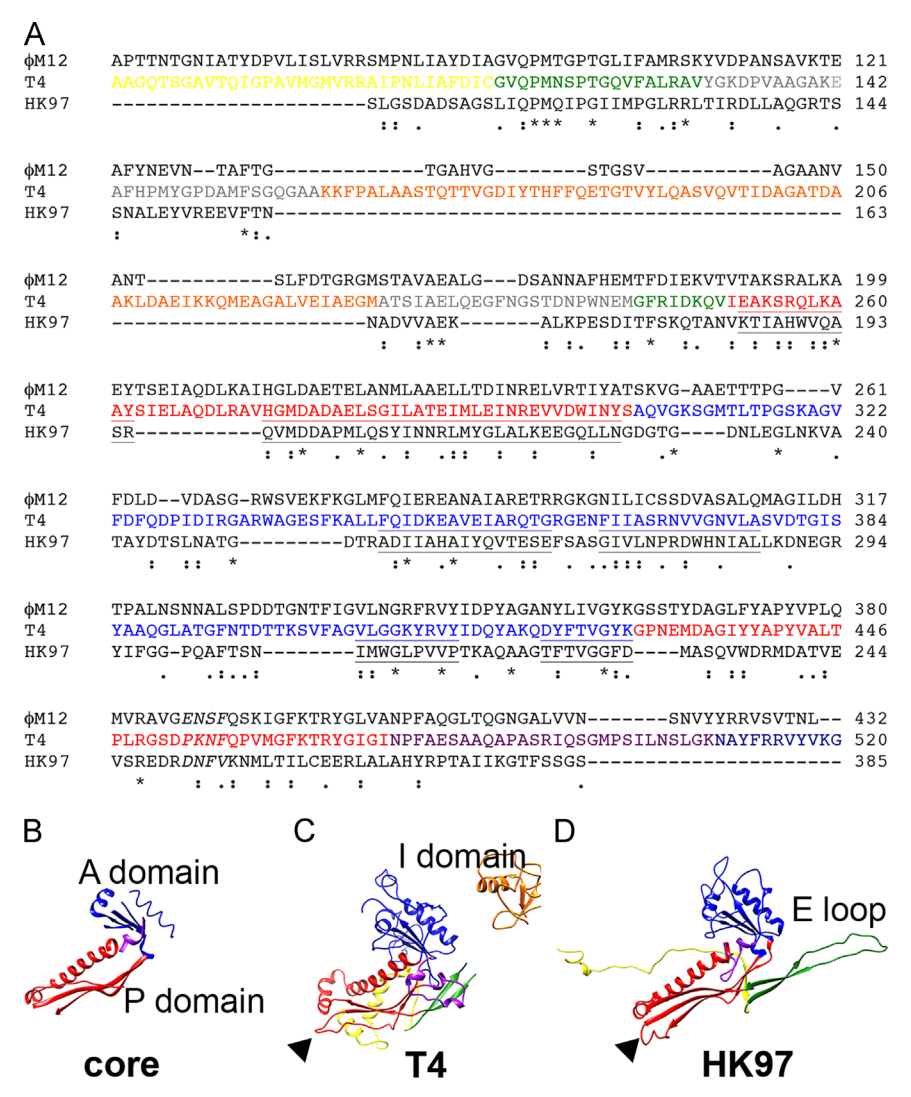


Fig. 5. (A) Alignment of ΦM12 gp23, T4 gp23, and HK97 gp5 shows clear homology. The T4 sequence and ribbon diagrams are colored by their domains: yellow=N-terminal; green=E-loop; orange=I domain; red=P domain; blue=A domain; purple=C-terminal. Elements that make up the core module are underlined and the elements that form the P-domain hairpin loop are in italics. "*" denotes identity, ":" denotes conserved, and "." denotes similar. (B) Core modules of the HK97-like major coat protein fold. (C) HK97 gp5 (PDB code 10HG (Helgstrand et al., 2003)) D. T4 gp24 (PDB code 1YUE (Fokine et al., 2005)). The arrow marks to location of the P-domain hairpin loop.

The core of the HK97 fold is created from two domains originally named because of their position relative to the 5- and quasi 6-fold axes, axial (A) and peripheral (P) (Wikoff et al., 2000) (Fig. 5). One variable region of the protein that is not included in this core contributes to structural stability of different phages in different ways. In HK97's major coat protein (gp5), a long β hairpin, the E loop, plays a special role by providing Lys169 that forms an isopeptide bond with Asn356 upon capsid maturation to stabilizes that capsid (Wikoff et al., 2000). This covalent stabilization is not universal and there is no evidence from denaturing gel electrophoresis analysis of the Φ M12 proteins that covalent modification stabilizes Φ M12's capsid (Brewer et al., in press). The T4 gp23 major capsid protein presents another variation at the E loop position because it has an additional chitin-binding-like insertion (I) domain (Fokine et al., 2005). This additional density contributes to the T4 phage head's spikey appearance and helps stabilize the capsid. Sequence analysis comparing the major capsid protein from ΦM12 to gp5 and gp23 from HK97 and T4, respectively, shows that Φ M12 gp23 diverges from both of these model systems at this region because it likely contains a significantly smaller I domain than T4 (Fig. 5). The flat ring of density at the pseudo 6-fold symmetry axis supports this prediction (Fig. 4E).

Close packing of the asymmetric hexamers could contribute to stability

In T4, the accessory protein Soc help the large I domain to stabilize the gp23/24 assembly (Steven et al., 1992). In HK97, covalent attachment of adjoining subunits stabilizes the mature coat (Duda et al., 1995). In Φ M12, there are no other ORFs that might correspond to an additional coat protein or known accessory factors like Soc. Further, the coat does not show any additional densities that might be attributed to unidentified accessory factors. Based on the genome, proteome and smooth surface of the coat, then, it appears that Φ M12 uses neither HK97's covalent chain mail nor T4's large I domain or accessory protein to stabilize its capsid shell.

In Φ M12, adjacent hexamers within the asymmetric unit are about 13 nm apart from one another whereas a pentamer and its adjacent hexamer are about 12 nm apart, forming a smooth, continuous coat. In T4, the average separation between neighboring hexamers is 14 nm, and between a hexamer and its neighboring pentamer is 13.5 nm (Fokine et al., 2004). In the T=7 Staphylococcus aureus-infecting 80 α , the mature capsid is marked by 2- to 3-nm holes that punctuate both the 2- and 3-fold

symmetry axes (Spilman et al., 2011). In contrast to both, the more closely placed hexamers and pentamers in Φ M12s capsid show continuous density at lower contours. Further, at higher contours, the pseudo 3-fold symmetry axis shows stronger density than at the pseudo 2-fold symmetry axis (Fig. 4D). The density at the pseudo 3-fold symmetry axis is filled by the hairpin loop in the P domain, another region of sequence variation between gp23 isoforms (Fig. 5A), suggesting this loop may be important in close packing of the T=191 hexamers.

Tails

2D averages of aligned tails from the base of the icosahedron to the tip of the tail show that both the collar and the baseplate have fewer features than the analogous elements in the enterobacteria T4 or cyanobacteria Syn9 phages (Fig. 5). In projection, the collar is straight and relatively short, running perpendicular to the long helical axis of the tail. Unlike T4, Φ M12 does not have the elaborate whisker/collar assembly that is quite prominent in the T4 neck. The identification of the protein(s) that could make up the perpendicular density seen at the Φ M12 neck remains unclear from the genome/proteomic analysis. Φ M12 does not contain a fibritin homolog; accordingly, the diffuse density seen at the top of the T4 tail is not seen in Φ M12. The three-layered baseplate has only weak traces of protruding density that correspond to the short, heterogeneous tail fibers, which are observable as variable densities in the raw images (Fig. 1). Unlike Syn9, the Φ M12 genome has few possible ORFs that could correspond to tail fibers of homologous sequence to other known tail fibers.

The baseplate of Φ M12 has fewer densities than its T4 cousin. Of the many baseplate proteins that have been characterized in T4, Φ M12's genome and proteome account for gp7, 8, 48, 5 and 26 and they could play analogous roles. One Φ M12 ORF with low homology to T4 gp12, the short tail fiber (STF), is represented in the proteomic analysis and could account for the diffuse density around the baseplate (Fig. 6). Interestingly, Φ M12 does not contain T4-homologous gp10, the anchor for the STFs (Leiman et al., 2006), or gp11, the interface for gp10 with the baseplate (Leiman et al., 2000), so the attachment mechanism of gp12-like protein likely relies on one of the uncharacterized, unique molecules identified in the proteomic analysis.

Empty capsid shell

The phage preparation resulted in a significant portion of capsids that were hollow inside. Refinement and reconstruction of those particles resulted in a T=19l icosahedron that was similar to the full capsid (Fig. 7). The empty capsid is about 5 nm wider than the full capsid, if measured from one icosahedral face to another, creating a somewhat bowed shell with round holes at the 2-fold symmetry axes. A similar empty form has been visualized in empty HK97 virions, where the bowed icosahedral faces of empty virions extend by about 8 nm from where they are when the DNA is packaged (Duda et al., 2009). This bowed, empty capsid is believed to be an intermediate on the way from the rounded balloon precursor to the packed, assembled capsid.

The presence of the tightly packed DNA inside a capsid creates a significant amount of pressure within the capsid, so one might anticipate that the DNA would exert pressure on the virion and cause it to bow. Rather, it appears that the DNA rigidifies the walls of the capsid, causing them to straighten up. Columns of density connect the center of the hexamers to the first ring of DNA (Fig. 4E), providing a possible mechanical means for this communication. In the absence of DNA, this density is not present and hexamers expand away from one another, causing the capsid to become porous (Fig. 7).

The same model of the hexamer fits into the star-shaped density in the empty shell, but each hexamer is rotated away from its

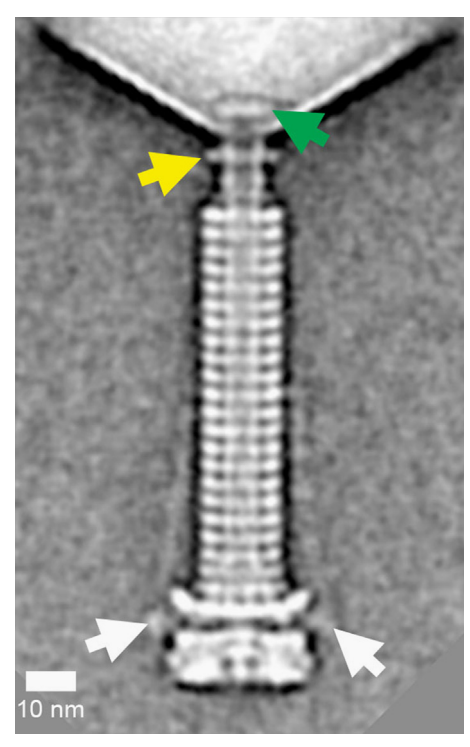


Fig. 6. 2D average of the helical tails shows a narrow neck and straight collar (yellow arrow), a density at the junction with the head (green arrow), and diffuse short tail fibers (white arrows). The scale bar is 10 nm.

neighbor relative to where it sits in the full capsid (Fig. 7C). The effect is to spread out and flatten the asymmetric unit at its 3-fold symmetry axis, leaving punctate holes in the capsid shell. The centers of the hexamers are separated by about 0.5 nm more than in the packed shells (hexamer–hexamer distance of 13 nm in the packed shell and hexamer–hexamer distance of 13.5 nm in the empty shell). As the hexamers separate, bowing the icosahedral face, the lower-density dimples that demarked the 2-fold in the full capsid become outright holes in the coat of the empty capsid (Fig. 7). Further, the pentamers, which previously sat quite high under the turrets, relax into the icosahedron. Interestingly, the turrets do not drop, but rather the connections between the turret and the pentamer thin, as if the protein that connects the turret to the penton is sufficiently flexible to absorb the relaxation (Fig. 3A, inset, and C, inset).

Conclusion

 Φ M12 is the first example of a novel icosahedral space group, T=19l, whose six hexamers and one pentamer subunit assemble in a fairly flat, dimpled capsid. Φ M12 has no obvious accessory proteins that stabilize the coat, and close interaction at the pseudo 3-fold symmetry axis ties together the asymmetric unit. This T4-superfamily bacteriophage has a contractile tail with a three-layered baseplate. Analysis of the T=19l geometry shows a particularly efficient packaging space. Without packed DNA, the icosahedron relaxes, maintaining essentially the same dimensions from turret tip to turret tip, but expanding at the icosahedral face.

Materials and methods

Phage purification

Phage was cultured as described elsewhere (Brewer et al., in press). The sample was heavily contaminated by *S. meliloti* proteins, including GroEL and flagella, but any attempt to further

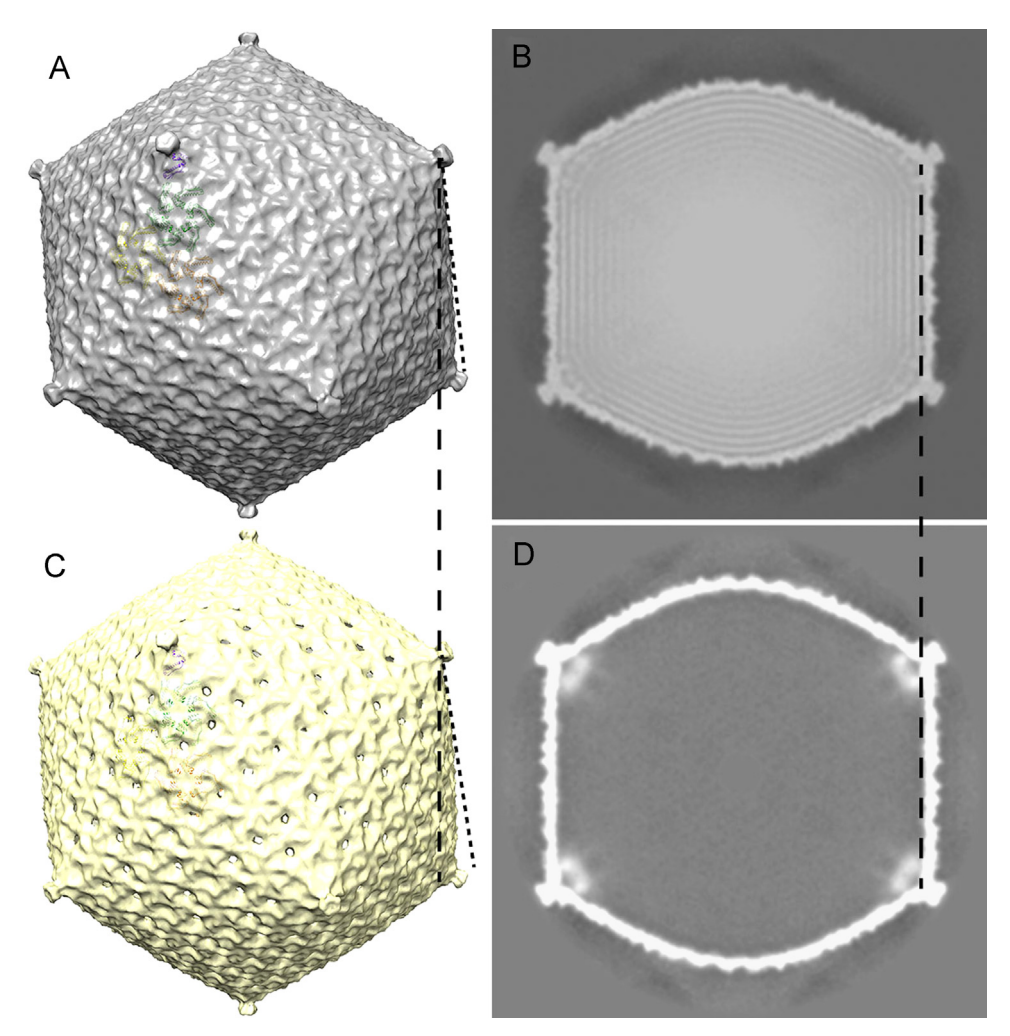


Fig. 7. (A) View down the 2-fold symmetry axis of the full Φ M12 capsid. (B) View down the 2-fold symmetry axis of the empty Φ M12 capsid The full and empty showing the similar T=19 surfaces that differ by only a few nm in diameter. The flat edge of the 3-fold, see in the full capsid, is bulged out in the empty particle and marked by a long dotted line in both representations. A shorter dotted line has been drawn in each surface to show the changing tangent of the face as the icosahedral face bows out. (C) The central slice of the full capsid. (D) The central slice of the empty capsid. The dotted line shows the slight bulging at the icosahedral face of the empty capsid.

purify the specimen by SDS-treatment, salt-treatment or sucrose-gradient fractionation reduced the infectivity and stability of phage samples (data not shown), so phage was subjected to minimal purification for cryo-EM. Chloroform-extracted phage was concentrated and washed on a 50 kD MWCO Amicon concentrator then resuspended at 3.6×10^8 infective particles/µL in $10\ mM$ sodium phosphate buffer (pH 7) and 1 mM MgSO₄ (phage buffer). The final preparation included full, partially packed, and empty capsids.

Preparation and plunge freezing of grids

Phage samples were initially screened in negative stain with an FEI CM120 transmission electron microscope (TEM) (FEI, Hillsboro, OR) and then prepared for cryogenic data collection using 2/2 Quantifoil holey carbon grids (SPI, West Chester, PA) discharged with the Solarus 950 Gatan Plasma Cleaner (Gatan, Pleasanton, CA). Samples were diluted 2-fold or 6-fold with phage buffer and plunge-frozen with the FEI Vitrobot Mark IV using blotting times of 3.5 or 4 s at 4 °C and 100% humidity.

Data collection and processing

For initial model building, tomographic tilt series were collected using the Leginon software (Carragher et al., 2000; Shrum

et al., 2012; Suloway et al., 2009) running on an FEI Titan Krios operating at 120 kV and equipped with a Gatan Tridem energy filtered CCD camera. Tilt series were aligned without fiducials and tomograms were calculated using Protomo 2.2 (Winkler and Taylor, 2006). Thirty-eight individual phage were windowed and Xmipp was used to align and then average the aligned subvolumes (Scheres et al., 2009). A scaled and filtered model of phage P22, an icosahedral short-tailed phage (Chang et al., 2006), was used as a reference for the alignment.

Single particle images were collected using the Leginon software (Carragher et al., 2000; Shrum et al., 2012; Suloway et al., 2009). Data were collected with a defocus range of -3.5 to $-1.5\,\mu m$, an electron dose of $15\,e-/\text{Å}^2$ on a Gatan $4k\times 4k$ Ultrascan 4000. The pixel size was calibrated to 1.35 Å/pixel at the specimen level, 65,555 times magnification, using images of graphitized carbon (Agar Scientific, Stansted, UK).

For the single particle data, 2717 packed and 2221 empty capsids were handpicked as two separate datasets. Partially packed capsids were also present but the internal density varied significantly, suggesting they were in different stages of DNA packaging or release, so were not reconstructed. Additionally, 376 fully extended tails were selected. The contrast transfer function (CTF) was corrected with the Automated CTF Estimation (ACE) function in Appion (Mallick et al., 2005). Next, each dataset was independently aligned, classified, and averaged, with EMAN,

Spider, and Xmipp, as implemented in Appion (Lander et al., 2009; Ludtke et al., 1999; Pascual-Montano et al., 2001). Refinement against two independently determined initial models yielded two structures with no detectable differences. The first initial model was calculated using the "starticos" module in EMAN (Ludtke et al., 1999). The second was taken from the low-resolution structure of the averaged tomograms. An advantage of the tomographic initial model was that it ensured that the refined model had the proper handedness. Within five rounds of alignment in EMAN, the structures converged and we continued refining in Frealign (Grigorieff, 2007) using a single model. The final reconstructions have a resolution of 1.8 nm (2038 particles in the final reconstruction) and 1.9 nm (1669 particles in the final reconstruction) at a Fourier shell correlation (FSC) of 0.5 for the full and empty capsids, respectively (Fig. S1).

Acknowledgments

We thank Scott Stagg for useful discussions and Brian Washburn, Christopher Stroupe, and Ann-Marie Torregrossa for reading the manuscript. This work was funded by USDA National Institute of Food and Agriculture, Agriculture and Food Research Initiative award 2010-65108-20582 to K.M.J, and American Heart Association award 10IRG4300065 to M.E.S. Molecular graphics and analyses were performed with the UCSF Chimera package. Chimera is developed by the Resource for Biocomputing, Visualization, and Informatics at the University of California, San Francisco (supported by NIGMS P41-GM103311). The EM volumes for both the full and empty shells have been deposited into the EMDB with the codes EMD-5717 and EMD-5718, respectively.

Appendix A. Supporting information

Supplementary data associated with this article can be found in the online version at http://dx.doi.org/10.1016/j.virol.2013.11.019.

References

- Adriaenssens, E.M., Van Vaerenbergh, J., Vandenheuvel, D., Dunon, V., Ceyssens, P.J., De Proft, M., Kropinski, A.M., Noben, J.P., Maes, M., Lavigne, R., 2012. T4-related bacteriophage LIMEstone isolates for the control of soft rot on potato caused by 'Dickeya solani'. PloS one 7. e33227.
- Brewer, T., Stroupe, M., Jones, K.. The genome and phylogenetic analysis of Sinorhizobium meliloti phage φM12, the founder of a new group of T4-like http://dx.doi.org/10.1016/j.virol.2013.11.027, in press.
- Carragher, B., Kisseberth, N., Kriegman, D., Milligan, R.A., Potter, C.S., Pulokas, J., Reilein, A., 2000. Leginon: an automated system for acquisition of images from vitreous ice specimens. J. Struct. Biol. 132, 33–45.
- Caspar, D.L., Klug, A., 1962. Physical principles in the construction of regular viruses. Cold Spring Harbor Symp. Quant. Biol. 27, 1–24.
- Chang, J., Weigele, P., King, J., Chiu, W., Jiang, W., 2006. Cryo-EM asymmetric reconstruction of bacteriophage P22 reveals organization of its DNA packaging and infecting machinery. Structure 14, 1073–1082.
- and infecting machinery. Structure 14, 1073–1082.

 Chen, C.R., Lin, C.H., Lin, J.W., Chang, C.I., Tseng, Y.H., Weng, S.F., 2007. Characterization of a novel T4-type Stenotrophomonas maltophilia virulent phage Smp14. Arch. Microbiol. 188, 191–197.
- Dreher, T.W., Brown, N., Bozarth, C.S., Schwartz, A.D., Riscoe, E., Thrash, C., Bennett, S.E., Tzeng, S.C., Maier, C.S., 2011. A freshwater cyanophage whose genome indicates close relationships to photosynthetic marine cyanomyophages. Environ. Microbiol. 13, 1858–1874.
- Duda, R.L., Hempel, J., Michel, H., Shabanowitz, J., Hunt, D., Hendrix, R.W., 1995. Structural transitions during bacteriophage HK97 head assembly. J. Mol. Biol. 247, 618–635.
- Duda, R.L., Ross, P.D., Cheng, N., Firek, B.A., Hendrix, R.W., Conway, J.F., Steven, A.C., 2009. Structure and energetics of encapsidated DNA in bacteriophage HK97 studied by scanning calorimetry and cryo-electron microscopy. J. Mol. Biol. 391, 471-483.
- Fokine, A., Chipman, P.R., Leiman, P.G., Mesyanzhinov, V.V., Rao, V.B., Rossmann, M. G., 2004. Molecular architecture of the prolate head of bacteriophage T4. Proc. Natl. Acad. Sci. U. S. A. 101, 6003–6008.

- Fokine, A., Leiman, P.G., Shneider, M.M., Ahvazi, B., Boeshans, K.M., Steven, A.C., Black, L.W., Mesyanzhinov, V.V., Rossmann, M.G., 2005. Structural and functional similarities between the capsid proteins of bacteriophages T4 and HK97 point to a common ancestry. Proc. Natl. Acad. Sci. U. S. A. 102, 7163–7168.
- Grigorieff, N., 2007. FREALIGN: high-resolution refinement of single particle structures. J. Struct. Biol. 157, 117–125.
- Helgstrand, C., Wikoff, W.R., Duda, R.L., Hendrix, R.W., Johnson, J.E., Liljas, L., 2003. The refined structure of a protein catenane: the HK97 bacteriophage capsid at 3.44 A resolution. J. Mol. Biol. 334, 885–899.
- Holmes, E.C., 2011. What does virus evolution tell us about virus origins? J. Virol. 85, 5247–5251.
- Lander, G.C., Stagg, S.M., Voss, N.R., Cheng, A., Fellmann, D., Pulokas, J., Yoshioka, C., Irving, C., Mulder, A., Lau, P.W., Lyumkis, D., Potter, C.S., Carragher, B., 2009. Appion: an integrated, database-driven pipeline to facilitate EM image processing. J. Struct. Biol. 166, 95–102.
- Leiman, P.G., Chipman, P.R., Kostyuchenko, V.A., Mesyanzhinov, V.V., Rossmann, M. G., 2004. Three-dimensional rearrangement of proteins in the tail of bacteriophage T4 on infection of its host. Cell 118, 419–429.
- Leiman, P.G., Kostyuchenko, V.A., Shneider, M.M., Kurochkina, L.P., Mesyanzhinov, V.V., Rossmann, M.G., 2000. Structure of bacteriophage T4 gene product 11, the interface between the baseplate and short tail fibers. J. Mol. Biol. 301, 975–985.
- Leiman, P.G., Shneider, M.M., Mesyanzhinov, V.V., Rossmann, M.G., 2006. Evolution of bacteriophage tails: Structure of T4 gene product 10. J. Mol. Biol. 358, 912–921.
- Ludtke, S.J., Baldwin, P.R., Chiu, W., 1999. EMAN: semiautomated software for high-resolution single-particle reconstructions. J. Struct. Biol. 128, 82–97.
- Mallick, S.P., Carragher, B., Potter, C.S., Kriegman, D.J., 2005. ACE: automated CTF estimation. Ultramicroscopy 104, 8–29.
- Mann, N.H., Clokie, M.R., Millard, A., Cook, A., Wilson, W.H., Wheatley, P.J., Letarov, A., Krisch, H.M., 2005. The genome of S-PM2, a "photosynthetic" T4-type bacteriophage that infects marine Synechococcus strains. J. Bacteriol. 187, 3188–3200.
- Miller, E.S., Kutter, E., Mosig, G., Arisaka, F., Kunisawa, T., Ruger, W., 2003.

 Bacteriophage T4 genome. Microbiol. Mol. Biol. Rev.: MMBR 67, 86–156. (table of contents)
- Pascual-Montano, A., Donate, L.E., Valle, M., Barcena, M., Pascual-Marqui, R.D., Carazo, J.M., 2001. A novel neural network technique for analysis and classification of EM single-particle images. J. Struct. Biol. 133, 233–245.
- Pettersen, E.F., Goddard, T.D., Huang, C.C., Couch, G.S., Greenblatt, D.M., Meng, E.C., Ferrin, T.E., 2004. UCSF Chimera–a visualization system for exploratory research and analysis. J. Comput. Chem. 25, 1605–1612.
- Scheres, S.H., Melero, R., Valle, M., Carazo, J.M., 2009. Averaging of electron subtomograms and random conical tilt reconstructions through likelihood optimization. Structure 17, 1563–1572.
- Shen, P.S., Domek, M.J., Sanz-Garcia, E., Makaju, A., Taylor, R.M., Hoggan, R., Culumber, M.D., Oberg, C.J., Breakwell, D.P., Prince, J.T., Belnap, D.M., 2012. Sequence and structural characterization of great salt lake bacteriophage CW02, a member of the T7-like supergroup. J. Virol. 86, 7907–7917.
- Shrum, D.C., Woodruff, B.W., Stagg, S.M., 2012. Creating an infrastructure for high-throughput high-resolution cryogenic electron microscopy. J. Struct. Biol. 180, 254–258.
- Spilman, M.S., Dearborn, A.D., Chang, J.R., Damle, P.K., Christie, G.E., Dokland, T., 2011. A conformational switch involved in maturation of Staphylococcus aureus bacteriophage 80alpha capsids. J. Mol. Biol. 405, 863–876.
- Steven, A.C., Greenstone, H.L., Booy, F.P., Black, L.W., Ross, P.D., 1992. Conformational changes of a viral capsid protein. Thermodynamic rationale for proteolytic regulation of bacteriophage T4 capsid expansion, co-operativity, and superstabilization by soc binding. J. Mol. Biol. 228, 870–884.
- Sullivan, M.B., Coleman, M.L., Weigele, P., Rohwer, F., Chisholm, S.W., 2005. Three Prochlorococcus cyanophage genomes: signature features and ecological interpretations. PLoS biology 3, e144.
- Sullivan, M.B., Huang, K.H., Ignacio-Espinoza, J.C., Berlin, A.M., Kelly, L., Weigele, P.R., DeFrancesco, A.S., Kern, S.E., Thompson, L.R., Young, S., Yandava, C., Fu, R., Krastins, B., Chase, M., Sarracino, D., Osburne, M.S., Henn, M.R., Chisholm, S.W., 2010. Genomic analysis of oceanic cyanobacterial myoviruses compared with T4-like myoviruses from diverse hosts and environments. Environ. Microbiol. 12, 3035–3056.
- Suloway, C., Shi, J., Cheng, A., Pulokas, J., Carragher, B., Potter, C.S., Zheng, S.Q., Agard, D.A., Jensen, G.J., 2009. Fully automated, sequential tilt-series acquisition with Leginon. J. Struct. Biol. 167, 11–18.
- Veesler, D., Cambillau, C., 2011. A common evolutionary origin for tailed-bacteriophage functional modules and bacterial machineries. Microbiol. Mol. Biol. Rev.: MMBR 75, 423–433. (first page of table of contents).
- Weigele, P.R., Pope, W.H., Pedulla, M.L., Houtz, J.M., Smith, A.L., Conway, J.F., King, J., Hatfull, G.F., Lawrence, J.G., Hendrix, R.W., 2007. Genomic and structural analysis of Syn9, a cyanophage infecting marine Prochlorococcus and Synechococcus, Environ. Microbiol. 9, 1675–1695.
- Wikoff, W.R., Liljas, L., Duda, R.L., Tsuruta, H., Hendrix, R.W., Johnson, J.E., 2000. Topologically linked protein rings in the bacteriophage HK97 capsid. Science 289, 2129–2133.
- Winkler, H., Taylor, K.A., 2006. Accurate marker-free alignment with simultaneous geometry determination and reconstruction of tilt series in electron tomography. Ultramicroscopy 106, 240–254.